Neurocomputing 106 (2013) 68–76

Contents lists available at SciVerse ScienceDirect

Neurocomputing

journal homepage: www.elsevier.com/locate/neucom

# Completed robust local binary pattern for texture classification

Yang Zhao [a,b], Wei Jia [c,*], Rong-Xiang Hu [c], Hai Min [a,b]

[a] Department of Automation, University of Science and Technology of China, Hefei 230027, China
[b] Institute of Intelligent Machines, Chinese Academy of Science, Hefei 230031, China
[c] Institute of Nuclear Energy Safety Technology, Chinese Academy of Science, Hefei 230031, China

ARTICLE INFO

*Article history:*
Received 6 April 2012
Received in revised form
14 October 2012
Accepted 29 October 2012
Communicated by: X. Li
Available online 15 November 2012

*Keywords:*
Local binary pattern
Texture classification

ABSTRACT

Original Local Binary Pattern (LBP) descriptor has two obvious demerits, i.e., it is sensitive to noise, and sometimes it tends to characterize different structural patterns with the same binary code which will reduce its discriminability inevitably. In order to overcome these two demerits, this paper proposes a robust framework of LBP, named Completed Robust Local Binary Pattern (CRLBP), in which the value of each center pixel in a $3 \times 3$ local area is replaced by its average local gray level. Compared to the center gray value, average local gray level is more robust to noise and illumination variants. To make CRLBP more robust and stable, Weighted Local Gray Level (WLG) is introduced to take place of the traditional gray value of the center pixel. The experimental results obtained from four representative texture databases show that the proposed method is robust to noise and can achieve impressive classification accuracy.



## 1. Introduction

Texture classification plays an important role in computer vision and image processing. In the past decades, numerous algorithms for texture feature extraction have been proposed, many of which focus on extracting texture features that are robust to noises, rotation and illumination variants [1]. Davis [2] exploited polarograms and generalized co-occurrence matrices to obtain rotation invariant statistical features. Duvernoy [3] proposed Fourier descriptors to extract texture feature on the spectrum domain. Goyal et al. [4] proposed a method by using texel property histogram. Eichmann and Kasparis [5] presented texture descriptors based on line structures extracted by Hough transform. Kashyap and Khotanzad [6] developed a circular simultaneous autoregressive (CSAR) model for rotation invariant texture classification. Cohen et al. [7] characterized texture as Gaussian Markov random fields and used the maximum likelihood to estimate rotation angles. Chen and Kundu [8] addressed rotation invariant by using multichannel sub-bands decomposition and hidden Markov model (HMM). Porter and Canagarajah [9] exploited the wavelet transform for texture classification by using the Daubechies four-tap wavelet filter coefficients. Recently, Varma and Zisserman [19,21,22] proposed to cluster a rotation invariant texton dictionary from a training set, and then form the textural histogram based on these textons. Later, Xu et al. [23–25] presented scale invariant texture classification methods by using a multi-fractal spectrum (MFS).

In [10], Ojala et al. proposed to use the Local Binary Pattern (LBP) for rotation invariant texture classification. As shown in Fig. 1, LBP code is computed by comparing a pixel with its neighbors. After the LBP code of each pixel in the image is defined, a histogram will be built to represent the texture image. LBP is a simple yet efficient operator to describe local texture, and has been proven to be invariant to monotonic gray scale transformations.

Since Ojala's work, a lot of variants of LBP have been proposed. For example, Heikkila et al. [11] proposed center-symmetric LBP (CS-LBP) by comparing center-symmetric pairs of pixels instead of comparing neighbors with central pixels. Liao et al. [12] presented Dominant LBP (DLBP), in which dominant patterns were experimentally chosen from all the patterns. Tan and Triggs [13] proposed Local Ternary Pattern (LTP), which extends original LBP to 3-valued codes. Guo et al. [14] proposed completed LBP (CLBP) by combining the conventional LBP with the measures of local intensity difference and central gray level. Recently, Khellah [15] presented a new method for texture classification, which combines Dominant Neighborhood Structure (DNS) and traditional LBP.

Although LBP and its variants have achieved impressive classification results on representative texture databases, there still remain some potential flaws of LBP. For example, LBP is sensitive to noise, and often classifies many different patterns into a same class. This paper attempts to solve these potential difficulties by proposing a robust framework of LBP, named Completed Robust Local Binary Pattern (CRLBP). In CRLBP, the value of each center pixel in a $3 \times 3$ local area is replaced by its average local gray level. Compared to gray value, average local gray level is more robust to noise and illumination variants. Experimental results illustrate that CRLBP achieves higher classification rates than other variants of LBP, and is insensitive to noise and illumination variants.

The rest of this paper is organized as follows: Section 2 briefly introduces two main flaws of LBP andtwo improved versions of LBP, i.e., LTP and CLBP. Section 3 presents the framework of

* Corresponding author.
*E-mail address:* icg.jiawei@gmail.com (W. Jia).

0925-2312/$ - see front matter © 2012 Elsevier B.V. All rights reserved.
http://dx.doi.org/10.1016/j.neucom.2012.10.017

CRLBP. Experimental results are reported in Sections 4 and Section 5 concludes the whole paper.

## 2. Related work

As we have mentioned above, the original LBP descriptor has some demerits. For example, LBP is sensitive to noise, and sometimes it tends to characterize different structural patterns with the same binary code, which will reduce its discriminability inevitably. Recently, in order to improve the original LBP, several new improved versions of LBP have been proposed including Local Ternary Pattern (LTP) [13] and Completed Local Binary Pattern (CLBP) [14]. In this section, we will briefly review two demerits of LBP and its two improved versions, i.e., LTP and CLBP.

### 2.1. Brief review of local ternary pattern (LTP)

Because the gray value of the central pixel is directly used as threshold, LBP is sensitive to noise, especially in the near-uniform image regions. As illustrated in Fig. 2, we can see that a little change of the central pixel (75–70) greatly affects the LBP code.

Aiming at this demerit, Tan and Triggs [13] extended original LBP to 3-valued LTP. The construction of LTP descriptor can be described by the following formula:

$$\mathrm{LTP}_{P,R}=\sum_{p=0}^{P-1}s\left(g_p-g_c\right)2^p,\quad s(x)=\begin{cases}1, & x\geq t\\ 0, & |x|<t\\ -1, & x<-t\end{cases} \tag{1}$$

where $g_c$ represents the gray value of the center pixel and $g_p(p=0,\ldots,P-1)$ denotes the gray value of the neighbor pixel on a circle of radius $R$, $P$ is the total number of the neighbors, and $t$ is a threshold specified by user. As being illustrated in Fig. 3, conventional 2-valued (0, 1) LBP code is extended to 3-valued ($-1$, 0, 1) ternary code by using the threshold $t$. Then the upper pattern and lower pattern are coded, respectively. LTP codes are more robust to noise, but no longer strictly invariant to monotonic gray scale transformation since threshold $t$ is specified by user.

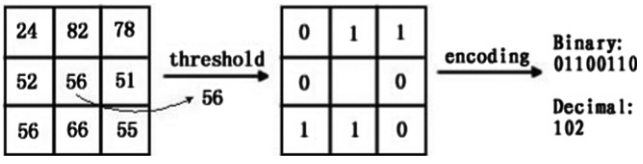


**Fig. 1.** Illustration of LBP process.

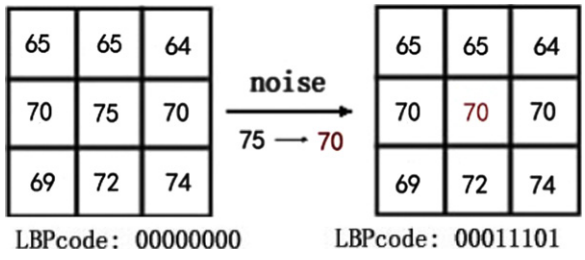


**Fig. 2.** An example that LBP is sensitive to noise.

### 2.2. Brief review of Completed LBP (CLBP)

Another demerit of LBP is that many different structural patterns may have the same LBP code. As shown in Fig. 4, pattern (a) and (b) have the same LBP code, but it is hard to say they have similar local structure.

In order to enhance the discriminative capability of the local structure, Guo et al. [14] proposed the method of CLBP. In CLBP, the image local differences are decomposed into two complementary components, i.e., the signs ($s_p$) and the magnitudes ($m_p$), respectively

$$s_p=s(g_p-g_c),\quad m_p|g_p-g_c| \tag{2}$$

where $g_p$, $g_c$ and $s(x)$ are defined as in Eq. (1). Two operators named CLBP-Sign (CLBP_S) and CLBP-Magnitude (CLBP_M) are proposed to

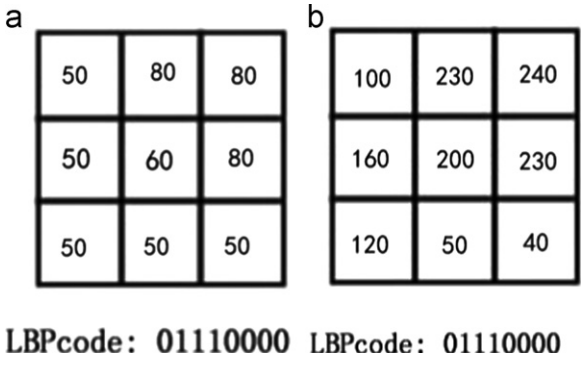


**Fig. 4.** An example that LBP characterize different structural patterns with the same binary code.

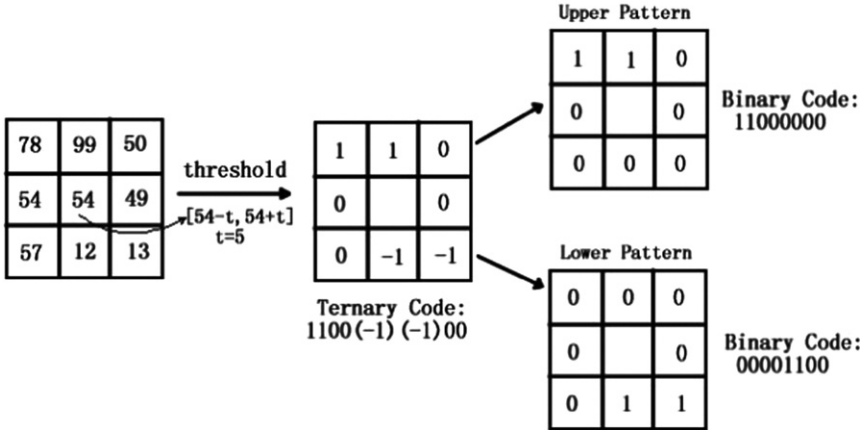


**Fig. 3.** Illustration of LTP ($P=8$, $R=1$).

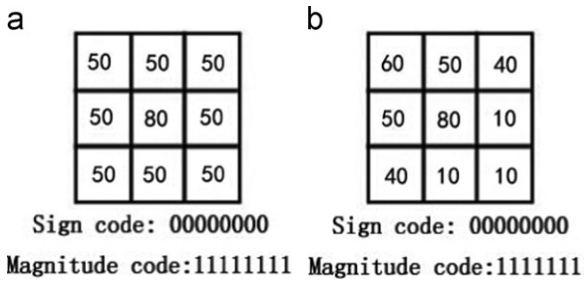


**Fig. 5.** Different patterns may have the same CLBP code.

code them, where CLBP_S is equivalent to the conventional LBP, and CLBP_M measures the local variance of magnitude. The CLBP_M can be defined as follows:

$$\mathrm{CLBP\_}M_{P,R}=\sum_{p=0}^{P-1}s(m_p-c)2^p,\quad s(x)=\begin{cases}1, & x\geq 0\\ 0, & x<0\end{cases} \tag{3}$$

where threshold $c$ is set as the mean value of $m_p$ of the whole image. Guo et al. observed that the center pixel also has discriminative information. Thus, they defined an operator named CLBP -Center (CLBP_C) to extract the local central information as follows:

$$\mathrm{CLBP\_}C_{P,R}=s(g_c-c_I) \tag{4}$$

where threshold $c_I$ is set as the average gray level of the whole image. By combining the three operators of CLBP_S, CLBP_M and CLBP_C, denoted as CLBP_S/M/C, significant improvement is made for differentiating the confusing patterns.

Although CLBP solves some confusion of different patterns, not all of these patterns can be differentiated perfectly. Fig. 5 illustrates an example that two patterns have the same signs code and magnitudes code (threshold $c=20$), but their local structures seem different to each other. Besides, it is obviously that CLBP is sensitive to noise since the value of a pixel is still used as a threshold directly.

## 3. Completed robust local binary pattern (CRLBP)

In order to solve the aforementioned difficulties, in this section, we propose a robust framework of LBP which inherits the merits of LTP and CLBP, but can overcome their flaws.

### 3.1. Robust local binary pattern (RLBP)

Aiming at finding a threshold which is insensitive to noise and invariant to monotonic gray scale transformation, we define the Average Local Gray Level (ALG) as follows:

$$\mathrm{ALG}=\frac{\sum_{i=1}^{8}g_i+g}{9} \tag{5}$$

where $g$ represents the gray value of the center pixel and $g_i(i=0,\ldots,8)$ denotes the gray value of the neighbor pixel. ALG represents the average gray level of local texture, which is obviously more robust to noise than the gray value of the central pixel. Then the LBP process is applied by using ALG as the threshold instead of the gray value, named Robust Local Binary Pattern (RLBP). As a result, we can define RLBP as follows:

$$\mathrm{RLBP}_{P,R}=\sum_{p=0}^{P-1}s(g_p-\mathrm{ALG}_c)2^p=\sum_{p=0}^{P-1}s\left(g_p-\frac{\sum_{i=1}^{8}g_{ci}+g_c}{9}\right)2^p \tag{6}$$

where $g_c$ represents the gray value of the center pixel and $g_p(p=0,\ldots,P-1)$ denotes the gray value of the neighbor pixel on a circle of radius $R$, $P$ is the total number of the neighbors, and $g_{ci}$ $(i=0,\ldots,8)$ denotes the gray value of the neighbor pixel of $g_c$. It is obviously that RLBP is insensitive to noise since average local gray level of pixel is used as a threshold. Besides, two different patterns with the same LBP code may have different RLBP code because that the neighbors of each neighbor pixel are also considered. Thus RLBP can overcome the aforementioned two demerits of original LBP.

ALG ignores the specific value of an individual pixel. While sometimes the specific information of the central pixel is needed. To make a balance between anti-noise and information of individual pixel, we define a Weighted Local Gray Level (WLG) as follows:

$$\mathrm{WLG}=\frac{\sum_{i=1}^{8}g_i+\alpha g}{8+\alpha} \tag{7}$$

where $g$ and $g_i$ are defined as in Eq. (5), $\alpha$ is a parameter set by user. It should be notice that WLG is equivalent to the conventional ALG if $\alpha$ is set as 1. Now the RLBP can be calculated as follows:

$$\mathrm{RLBP}_{P,R}=\sum_{p=0}^{P-1}s(g_p-\mathrm{WLG}_c)2^p=\sum_{p=0}^{P-1}s\left(g_p-\frac{\sum_{i=1}^{8}g_{ci}+\alpha g_c}{8+\alpha}\right)2^p \tag{8}$$

where $g_p$, $g_c$, $g_{ci}$ are defined as in Eq. (6), $\alpha$ is the parameter of WLG. A set of experiments were carried out on a large texture database to select the optimal parameter $\alpha$ in this paper. The images in the CUReT database were captured under significantly illumination changes, viewpoint variants, and scales transformations. Thus, the experimental setup was conducted on the CUReT database and noisy CUReT database (SNR=5), which will be discussed later in Section 4.3. The response functions of different parameter $\alpha$ on CUReT database and noisy CUReT database are illustrated in Fig. 6. As illustrated in Fig. 6(a), RLBP performs better when $\alpha$ is set as 8, 9, 10 on normal database. Fig. 6(b) shows that RLBP performs best in anti-noise when $\alpha$ is set as 1, and RLBP will be more sensitive to noise if $\alpha$ is set larger than 8. Thus, in our approach, $\alpha$ is set as 1 or 8 according to experimental results. In other words, RLBP ($\alpha=1$) is more insensitive to noise than RLBP ($\alpha=8$), while RLBP ($\alpha=8$) performs more stably under complex illumination and viewpoint variant conditions, since it extracts the gray level information of both local neighbor set and individual pixel.

### 3.2. Completed robust local binary pattern (CRLBP)

For differentiating the confusing patterns of LBP, RLBP inherits the effective framework of CLBP. The magnitude $m_p$ is usually defined as follows:

$$m_p=\left|\mathrm{WLG}_p-\mathrm{WLG}_c\right|=\left|\frac{\sum_{i=1}^{8}g_{pi}+\alpha g_p}{8+\alpha}-\frac{\sum_{i=1}^{8}g_{ci}+\alpha g_c}{8+\alpha}\right| \tag{9}$$

where $g_p$, $g_c$, $g_{ci}$ are defined as in Eq. (6), $g_{pi}$ $(i=0,\ldots,8)$ denotes the gray value of the neighbor pixel of $g_p$, and $\alpha$ is the parameter of WLG. RLBP-Magnitude (RLBP_M) measures the local variance of WLG. As a result, we define RLBP_M as follows:

$$\mathrm{RLBP\_}M_{P,R}=\sum_{p=0}^{P-1}s(m_p-c)2^p \tag{10}$$

where threshold $c$ is set as the mean value of $m_p$ of the whole image. The center pixel, which expresses the image central gray level, also has discriminative information. Thus, we also defined an operator named RLBP-Center (RLBP_C) to extract the local central information as follows:

$$\mathrm{RLBP\_}C_{P,R}=s(\mathrm{WLG}_c-c_I) \tag{11}$$

where threshold $c_I$ is set as the average local gray level of the whole image. As in [14], we use the same way to combine the three operators of RLBP, RLBP_M and RLBP_C, denoted as CRLBP.

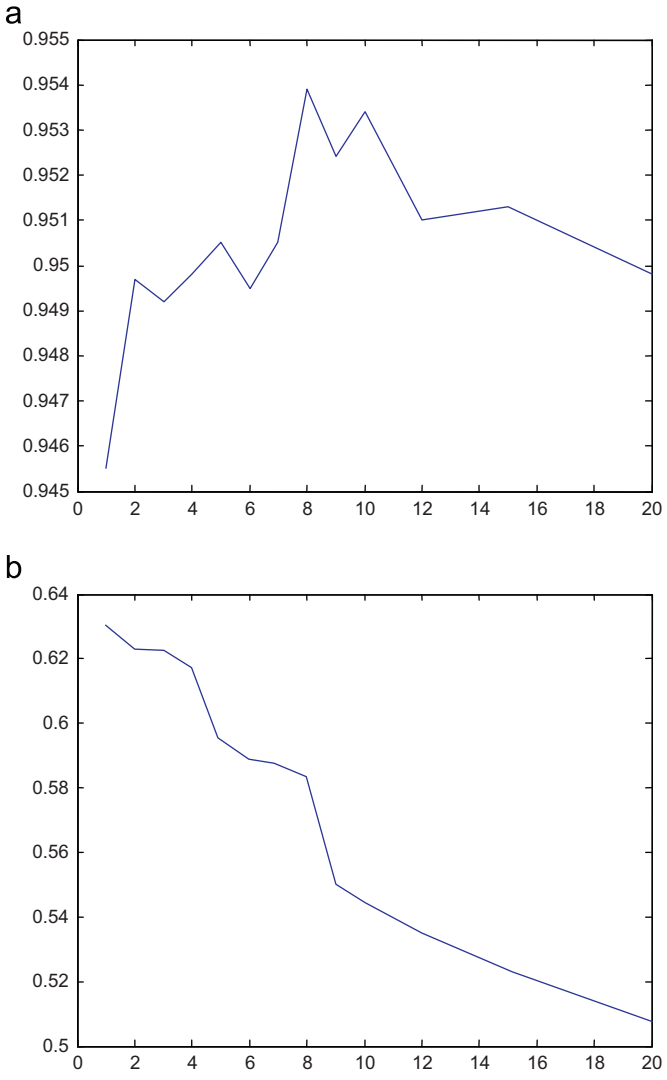


**Fig. 6.** Texture classification rates under different values of $\alpha$ (0–20). (a) The classification rates on CUReT database with $R=1$, $P=8$, and 46 training samples and (b) the classification rates on noisy CUReT database with $R=1$, $P=8$, SN$R=5$, and 46 training samples.

### 3.3. Dissimilarity measure

Several measures have been proposed for discriminating the dissimilarity between two histograms. In this paper, we utilize the $\chi^2$ statistics to address the problem. If $H=\{h_i\}$ and $K=\{k_i\}$ $(i=1, 2\ldots B)$ denote two histograms, then *the* $\chi^2$ statistics can be calculated as follows:

$$d_{\chi^2}(H,K)=\sum_{i=1}^{B}\frac{(h_i-k_i)^2}{h_i+k_i} \tag{12}$$

In this paper, assuming that all the methods used the nearest neighborhood classifier for classification.

## 4. Experimental results

To evaluate the effectiveness of the proposed method, we carried out a series of experiments on four representative texture databases, i.e., the Outex database [16], the UIUC database [17], the CUReT database [18], and the XU_HR database [26]. The first set of experiments is conducted on Outex database and follows the experimental setup in [14]. The second set of experiments is performed on the UIUC database. For experiments conducted on noisy images, each texture image was corrupted by additive Gaussian noise with zero mean and standard deviation that was determined according to the corresponding Signal-to-Noise Ratios (SNR) value. The third set of experiments is conducted on the CUReT database. The experimental setup is similar to the one presented in [14,20]. The last experiment is performed on the XU High Resolution database.

### 4.1. Experimental results on Outex database

When conducting the experiments on the Outex database (see Fig. 7), we used the Outex test suits Outex_TC_0010 (TC10) and Outex_TC_0012 (TC12), where TC10 and TC12 contain 24 classes of texture images captured under three illuminations ("inca", "tl84" and "horizon") and nine rotation angles (0°, 5°, 10°, 15°, 30°, 45°, 60°, 75°, and 90°). There are twenty $128\times128$ images for each rotation angle under a given illumination condition. The $24\times20$ images of illumination "inca" and rotation angle 0° were adopted as the training data. For TC10 dataset the other eight rotation angles with illumination "inca" are used for test. For TC12 dataset, all the $24\times20\times9$ samples

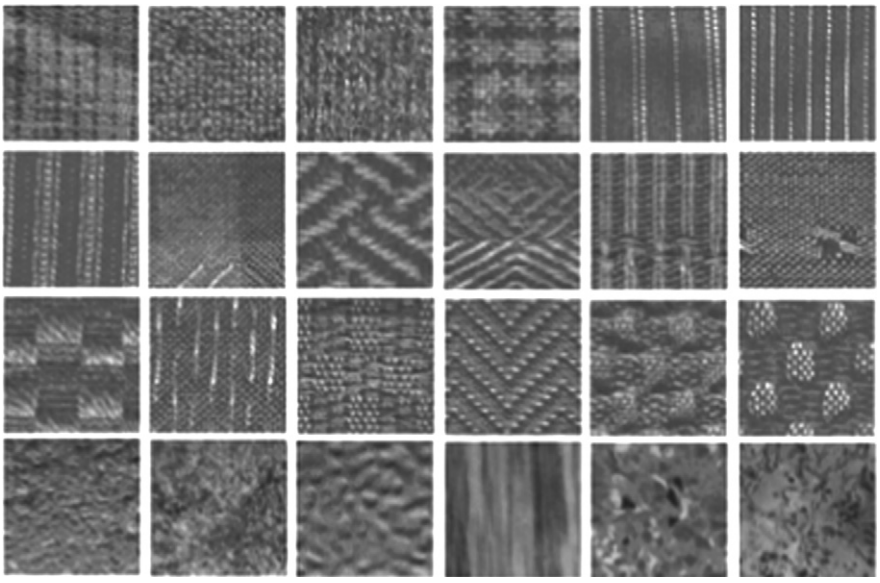

**Fig. 7.** 24 texture images from the Outex database.

captured under illumination "tl84" or "horizon" were used as the test data.

For the experiments on the Outex database, the performance of our approach is compared with several other methods including original LBP [10], LTP [13], DLBP [12], CLBP [14], and DNS+LBP [15]. Table 1 lists the experimental results of different methods, from which we could make the following findings. First, except for the experiment ($R=2$, $P=16$) on TC10 dataset, CRLBP performs much better than other methods. It should be noticed that CRLBP ($\alpha=8$) achieves better results under illumination "tl84" and "horizon" than other methods, that demonstrates CRLBP ($\alpha=8$) is more robust to illumination variations. Second, similar conclusion can be made to CRLBP ($\alpha=1$). CRLBP ($\alpha=1$) performs better than other variants of LBP on average, especially under different illuminations. Finally,

**Table 1**
Classification rate (%) on Outex TC10 and TC12 datasets.

| | $R=1$, $P=8$ | | | | $R=2$, $P=16$ | | | | $R=3$, $P=24$ | | | |
|---|---|---|---|---|---|---|---|---|---|---|---|---|
| | TC10 | TC12 | | Average | TC10 | TC12 | | Aver-age | TC10 | TC12 | | Average |
| | | t184 | Horizon | | | tl84 | Horizon | | | tl84 | Horizon | |
| LBP | 84.81 | 65.46 | 63.68 | 71.31 | 89.40 | 82.26 | 75.20 | 82.28 | 95.07 | 85.04 | 80.78 | 86.96 |
| LTP | 93.39 | 73.94 | 72.89 | 80.07 | 96.20 | 87.85 | 83.38 | 89.14 | 97.71 | 90.74 | 85.65 | 91.37 |
| CLBP_M | 81.74 | 59.30 | 62.77 | 67.93 | 93.67 | 73.79 | 72.40 | 79.95 | 95.52 | 81.18 | 78.65 | 85.11 |
| CLBP_S/M/C | 96.56 | 90.30 | 92.29 | 93.05 | 98.72 | 93.54 | 93.91 | 95.39 | 98.93 | 95.32 | 94.53 | 96.26 |
| RLBP ($\alpha=8$) | 83.96 | 73.17 | 63.82 | 73.65 | 89.27 | 84.54 | 79.93 | 84.58 | 94.30 | 84.58 | 82.52 | 87.13 |
| RLBP_M ($\alpha=8$) | 85.26 | 66.41 | 66.16 | 72.61 | 93.88 | 76.39 | 78.63 | 82.97 | 96.12 | 80.07 | 81.39 | 85.86 |
| CRLBP ($\alpha=8$) | **97.55** | **91.94** | **92.45** | **93.98** | 98.59 | 95.88 | 96.41 | 96.96 | 99.35 | 96.83 | 96.16 | 97.45 |
| RLBP ($\alpha=1$) | 84.43 | 80.74 | 76.90 | 80.69 | 92.34 | 88.08 | 86.02 | 88.81 | 92.32 | 83.98 | 83.36 | 86.55 |
| RLBP_M ($\alpha=1$) | 85.23 | 66.76 | 67.62 | 73.20 | 94.58 | 78.45 | 81.74 | 84.92 | 96.97 | 80.72 | 82.18 | 86.62 |
| CRLBP ($\alpha=1$) | 96.54 | 91.16 | 92.06 | 93.25 | 98.85 | **96.67** | **96.97** | **97.50** | **99.48** | **97.57** | **97.34** | **98.13** |
| DNS+LBP[15] | – | – | – | – | **98.90** | 93.22 | 92.13 | 94.75 | 99.27 | 94.40 | 92.85 | 95.51 |
| DLBP +NGF[12] | TC10:99.1 TC12:'tl84'93.2 and 'horizon'90.4 | | | | | | | | | | | |

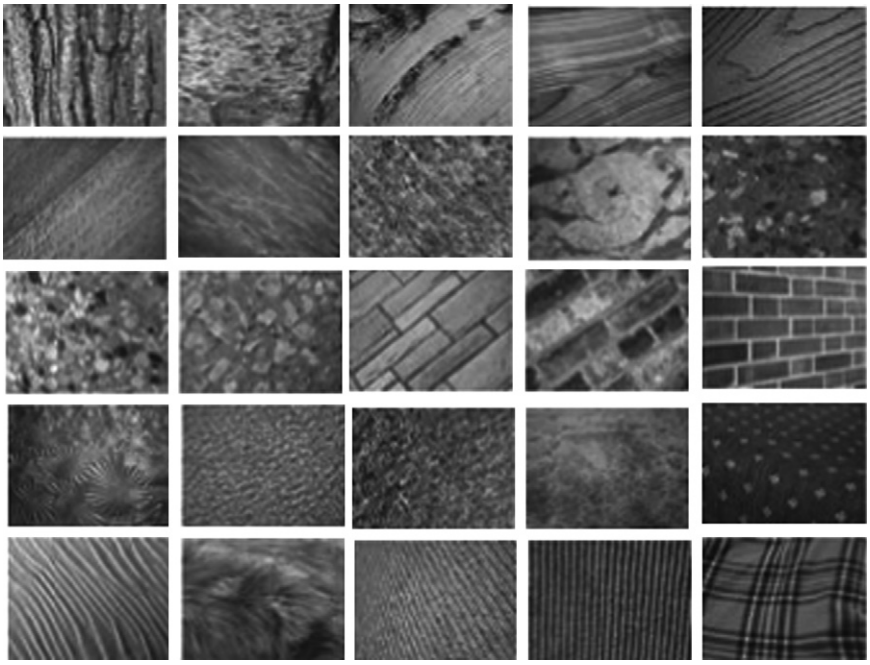

**Fig. 8.** 25 texture images from the UIUC database.

**Table 2**
Classification rate (%) on UIUC database.

| | $R=1$, $P=8$ | | | | $R=2$, $P=16$ | | | | $R=3$, $P=24$ | | | |
|---|---|---|---|---|---|---|---|---|---|---|---|---|
| | 20 | 15 | 10 | 5 | 20 | 15 | 10 | 5 | 20 | 15 | 10 | 5 |
| LBP | 54.65 | 52.94 | 47.14 | 39.72 | 61.32 | 56.42 | 51.16 | 42.03 | 64.67 | 60.05 | 54.25 | 44.59 |
| CLBP_S/M/C | 87.64 | 85.70 | 82.65 | 75.05 | 91.04 | 89.42 | 86.29 | 78.57 | 91.19 | 89.21 | 85.95 | 78.05 |
| RLBP ($\alpha=8$) | 61.68 | 59.26 | 53.95 | 44.98 | 65.99 | 62.46 | 56.73 | 48.19 | 68.09 | 64.83 | 59.84 | 50.28 |
| CRLBP ($\alpha=8$) | **88.01** | **86.62** | **82.97** | **76.01** | 91.99 | 90.41 | 88.04 | 81.49 | 92.83 | 90.55 | 88.02 | 80.54 |
| RLBP ($\alpha=1$) | 65.41 | 63.18 | 58.71 | 51.38 | 68.06 | 65.06 | 60.37 | 51.25 | 72.79 | 69.54 | 64.03 | 53.04 |
| CRLBP ($\alpha=1$) | 86.91 | 85.67 | 82.20 | 73.95 | **92.92** | **91.82** | **88.15** | **81.98** | **93.31** | **92.03** | **89.47** | **81.90** |

compared CRLBP ($\alpha=8$) with CRLBP ($\alpha=1$), the former one performs best when radius is 1, and the latter one achieves the highest classification rates at other radius. In one word, CRLBP can get higher classification rates than other methods and it is more insensitive to illumination variations.

### 4.2. Experimental results on UIUC database

The UIUC texture database (see Fig. 8) includes 25 classes and 40 images in each class. The resolution of each image is $640 \times 480$. The database contains materials imaged under significant viewpoint variations. To assess classification performance, $N$ training images are randomly chosen from each class while the remaining 40-$N$ images are used as the test set. The average accuracy over 100 randomly splits are listed in Table 2.

Similar findings to those in section 4.1 can be found in Table 2. First, CRLBP ($\alpha=8$) achieves better results than CLBP at any condition. Second, CRLBP ($\alpha=1$) performs much better than CLBP when the radius is larger than one, but it performs worse than CLBP at ($R=1$, $P=8$). Finally, compared CRLBP ($\alpha=8$) with CRLBP ($\alpha=1$), the former one performs best at ($P=1$, $R=8$), and the latter one achieves the highest classification rates at other radius.

For experiments conducted on noisy UIUC texture images, 20 training images are randomly chosen from each class. The partition is also implemented over 100 times independently with ($P=3$, $R=24$). The average results on the noisy images are listed in Table 3.

From Table 3, we can easily found that CRLBP ($\alpha=1$) is most robust to noise. CRLBP ($\alpha=1$) performs 2.75% higher than CLBP when SNR value is 100, and it achieves 11.66% higher than CLBP when SNR value is 5. As analyzed in Section 3.1, same conclusion can be made from Tables 2 and 3. CRLBP ($\alpha=1$) and CRLBP ($\alpha=8$) perform better than CLBP, and CRLBP ($\alpha=1$) is most insensitive to noise.

**Table 3**
Classification rate (%) on UIUC database with additive Gaussian noise of different Signal-To-Noise Ratios (SNR).

| ($R=3$, $R=24$ and $N=20$) | SNR 100 | SNR 30 | SNR 15 | SNR 10 | SNR 5 |
|---|---|---|---|---|---|
| CLBP | 90.74 | 90.38 | 87.56 | 81.64 | 67.54 |
| CRLBP ($\alpha=8$) | 92.51 | 92.28 | 91.11 | 85.90 | 77.16 |
| CRLBP ($\alpha=1$) | **93.49** | **93.08** | **92.74** | **88.57** | **79.20** |

### 4.3. Experimental results on CUReT database

The CUReT database includes 61 classes of textures captured at different viewpoints and illumination orientations (see Fig. 9). In each class, 92 images are selected from the images shot from a viewing angle of less than 60°. As in [14,19], $N$ images were randomly chosen as training samples from each class. The remaining 92-$N$ images were used as test samples. The average classification rates over 100 random splits are listed in Table 4.

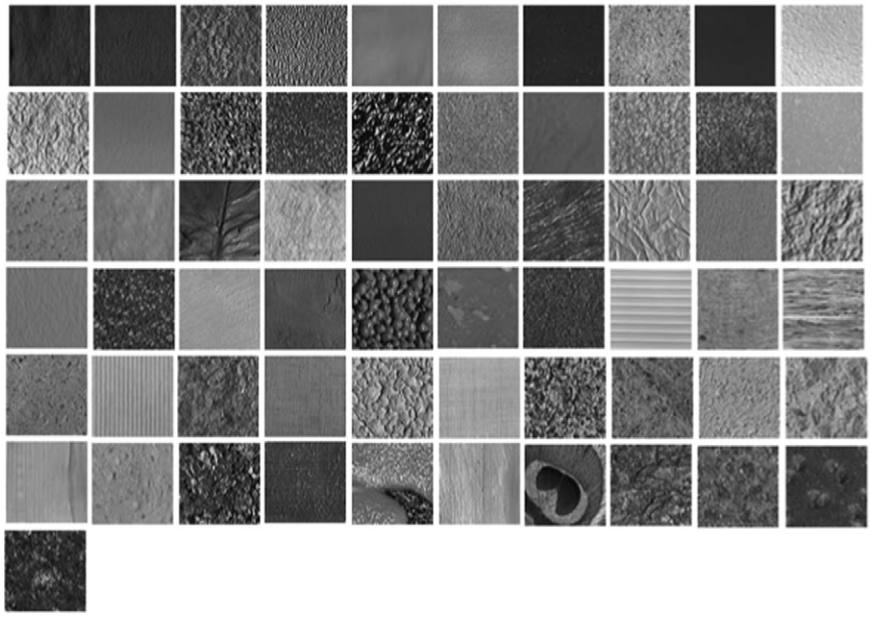

**Fig. 9.** 61 texture images from the CUReT database.

**Table 4**
Classification rate (%) on CUReT database.

| | $R=1$, $P=8$ | | | | $R=2$, $P=16$ | | | | $R=3$, $P=24$ | | | |
|---|---|---|---|---|---|---|---|---|---|---|---|---|
| | 46 | 23 | 12 | 6 | 46 | 23 | 12 | 6 | 46 | 23 | 12 | 6 |
| LBP | 79.93 | 74.40 | 67.62 | 58.05 | 76.19 | 70.39 | 64.27 | 56.30 | 79.47 | 73.72 | 67.62 | 59.81 |
| CLBP_S/M/C | 95.19 | 91.20 | 83.81 | 73.44 | 95.35 | 91.24 | 84.66 | 75.41 | 95.38 | 91.77 | 85.01 | 76.16 |
| RLBP ($\alpha=8$) | 74.13 | 68.75 | 62.15 | 54.09 | 76.19 | 70.39 | 64.27 | 56.30 | 79.47 | 73.72 | 67.62 | 59.81 |
| CRLBP ($\alpha=8$) | **95.39** | **91.33** | **85.40** | **76.56** | **95.88** | **91.85** | **86.44** | **77.79** | **96.27** | **91.83** | **86.06** | **78.43** |
| RLBP ($\alpha=1$) | 71.63 | 66.24 | 60.49 | 53.44 | 72.10 | 66.35 | 60.26 | 53.13 | 74.05 | 68.18 | 61.98 | 54.50 |
| CRLBP ($\alpha=1$) | 94.55 | 89.47 | 82.72 | 73.22 | 94.78 | 91.10 | 85.47 | 76.39 | 95.35 | 90.73 | 85.05 | 76.34 |
| DNS+LBP[15] | – | – | – | – | 95.00 | – | – | – | 94.52 | – | – | – |

We could get the following observation from Table 4. First, CRLBP ($\alpha=8$) achieves higher classification rates than other methods, especially when the training samples are less than 23. Second, CRLBP ($\alpha=1$) performs worse than CLBP on this database when the training samples are enough. When the training samples are less than 23 and radius are larger than 1, CRLBP ($\alpha=1$) perform slightly better than CLBP. Thus, CRLBP ($\alpha=8$) is more stable than CRLBP ($\alpha=1$) since it extracts both local gray level information and the specific information of individual pixel.

For experiments conducted on noisy CUReT texture images, 46 images are randomly chosen from each class as train samples. The partition is also implemented over 100 times independently with ($P=3$, $R=24$). The average results on the noisy images are listed in Table 5.

When it is come to noisy images, we can get the following finding from Table 5. First, CRLBP ($\alpha=8$) still achieve higher classification accuracy than CLBP. Second, although CRLBP ($\alpha=1$) performs worse than CLBP on normal images, it get much better results on noisy datasets.

**Table 5**
Classification rate (%) on CUReT database with additive Gaussian noise of different Signal-To-Noise Ratios (SNR).

| ($R=3$, $R=24$ and $N=46$) | SNR 100 | SNR 30 | SNR 15 | SNR 10 | SNR 5 |
|---|---|---|---|---|---|
| CLBP | 95.51 | 95.87 | 87.23 | 72.77 | 51.35 |
| CRLBP ($\alpha=8$) | **96.34** | **96.18** | 92.30 | 82.88 | 64.97 |
| CRLBP ($\alpha=1$) | 96.06 | 95.90 | **93.56** | **85.58** | **69.67** |

### 4.4. Experimental results on XU_HR database

The XU High Resolution texture database (see Fig. 10) includes 25 classes and 40 images in each class. The resolution of each image is $1280\times960$. The images in this database are with very large resolution variations. To assess classification performance, $N$ training images are randomly chosen from each class while the remaining 40-$N$ images are used as the test set. The average accuracy over 100 randomly splits are listed in Table 6.

We could make the following findings from Table 6. First, CRLBP ($\alpha=8$) performs best when the radius is larger than 1. Second, CRLBP ($\alpha=1$) achieves higher classification rates when the radius is 1. Last, it also should be notice that CLBP performs better when $R=1$, $P=8$, 5 training samples. But CRLBP is better than CLBP at any other conditions.

### 4.5. Compared with recent non-LBP methods

The LBP and its variants use specified structural patterns to form texture histogram. Instead of using the fixed texture patterns, Verma and Zisserman [21] proposed to cluster the textons by using the max responses of several filters (VZ_MR8). Later, they [22] presented a new texton dictionary clustered by using the image local patch. In [19], they proposed to find a dominant orientation of the local patch to address the rotation invariant issue (VZ_Joint). In these aforementioned works, the spatial information of how pixels are distributed is lost. Aiming at this demerit of the global texture descriptors, Xu et al. [23] proposed a scale invariant texture feature

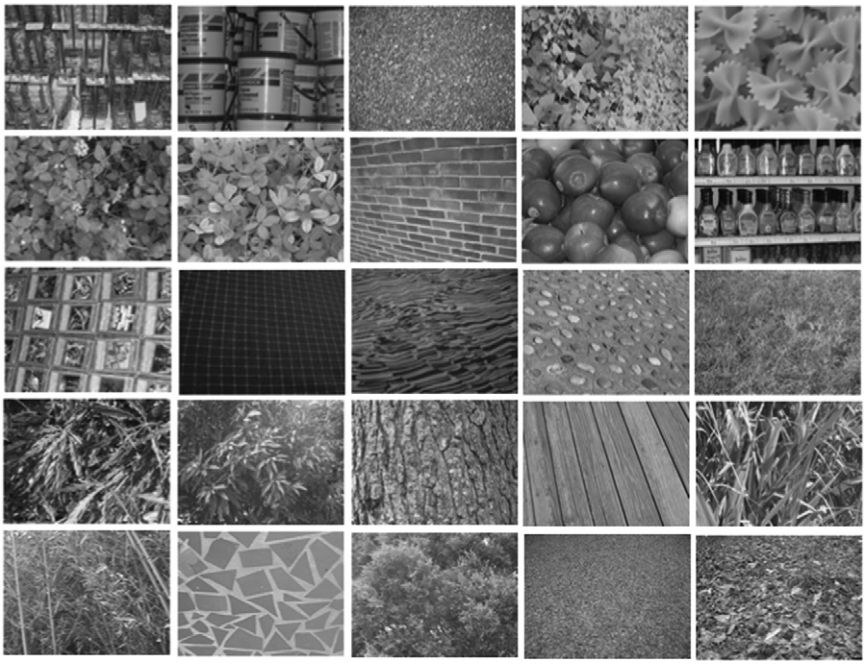

**Fig. 10.** 25 texture images from the XU_HR database.

**Table 6**
Classification rate (%) on XU_HR database.

| | $R=1$, $P=8$ | | | | $R=2$, $P=16$ | | | | $R=3$, $P=24$ | | | |
|---|---|---|---|---|---|---|---|---|---|---|---|---|
| | 20 | 15 | 10 | 5 | 20 | 15 | 10 | 5 | 20 | 15 | 10 | 5 |
| CLBP_S/M/C | 96.20 | 95.54 | 94.39 | **91.35** | 97.34 | 96.73 | 95.38 | 91.10 | 97.73 | 96.65 | 95.17 | 91.59 |
| CRLBP ($\alpha=8$) | 95.32 | 93.79 | 91.98 | 86.18 | **98.37** | **97.30** | **96.41** | 92.73 | **98.22** | **97.51** | **96.51** | **92.91** |
| CRLBP ($\alpha=1$) | **96.31** | **95.63** | **94.45** | 89.81 | 98.06 | 97.27 | 96.11 | **92.89** | 98.12 | 97.34 | 95.82 | 92.34 |

**Table 7**
Classification rates (%) of different methods on three databases.

| | Outex database | | | | CUReT database | | | | UIUC database | | | |
|---|---|---|---|---|---|---|---|---|---|---|---|---|
| | TC10 | "tl84" | "horizon" | Average | 46 | 23 | 12 | 6 | 20 | 15 | 10 | 5 |
| CRLBP ($\alpha=1$) | **99.48** | **97.57** | 97.34 | **98.13** | 95.35 | 90.73 | 85.05 | 76.34 | 93.31 | 92.03 | 89.47 | 81.90 |
| CRLBP ($\alpha=8$) | 99.35 | 96.83 | 96.16 | 97.45 | 96.27 | 91.83 | 86.06 | 78.43 | 92.83 | 90.55 | 88.02 | 80.54 |
| VZ_Joint | 98.51 | 97.45 | **98.35** | 98.10 | 96.51 | 93.42 | 88.22 | 79.14 | 93.27 | 92.00 | 88.39 | 80.87 |
| VZ_MR8 | 94.06 | 92.61 | 93.31 | 93.32 | **97.86** | **95.54** | **91.28** | **83.46** | 93.96 | 92.68 | 89.32 | 83.07 |
| MFS+SVM [25] | – | – | – | – | – | – | – | – | 92.74 | 91.38 | 88.36 | 82.24 |
| WMFS+SVM[25] | – | – | – | – | – | – | – | – | **98.60** | **98.01** | **96.95** | **93.42** |

by using the multi-fractal spectrum (MFS). Recently, Xu et al. [25] presented a new descriptor based on multi-fractal analysis in wavelet pyramids of texture images (WMFS).

The performance of the proposed CRLBP ($R=3$, $P=24$) is compared with that of these non-LBP methods. The experimental results of MFS and WMFS on UIUC database are from [25]. The Chi-square dissimilarity defined in Section 3.3 and the nearest neighborhood classifier are used for all other methods here. The experimental results on three texture databases are listed in Table 7.

We could make the following findings from Table 7. First, the CRLBP achieves similar classification rate to VZ_Joint on these databases. It should be noticed that the VZ_Joint requires a texton generation process, which often cost several hours. While the CRLBP is computationally efficient since it does not require texton generation step. By the same hardware the CRLBP takes 50 ms, while VZ_Joint spends about 700 s to build a texture histogram for one image. Thus, the CRLBP is much more efficient than VZ_Joint. Second, compared the CRLBP with VZ_MR8, the CRLBP performs better than VZ_MR8 on Outex database, and the VZ_MR8 performs slightly better on other databases. Similar to VZ_Joint, VZ_MR8 also need to cluster the textons from the training set, and total 38 filters are used in the MR8 filter bank. Compared to VZ_MR8, the CRLBP is more simple and faster. Third, the MFS is proved to be robust to view-point changes [24] and it performs impressively on the UIUC database which contains materials imaged under significant viewpoint variations. Both the CRLBP and the MFS are computation efficient, and their performances on the UIUC database are also similar to each other. Last, WMFS performs much better than other methods on the UIUC database. It also should be noticed that the scales of the images are normalized before the multi-orientation wavelet pyramid multi-fractal analysis in WMFS [25]. The scale estimation and normalization step can greatly enhance the performance of the WMFS, which is not applied in other methods. In one word, the CRLBP can achieve comparable classification rate to other recent non-LBP texture classification methods except the WMFS on the UIUC database.

## 5. Conclusions

In this paper, we studied the two main demerits of Local Binary Pattern (LBP), and then we proposed a new robust framework of LBP, named Completed Robust Local Binary Pattern (CRLBP). In order to make a balance of robustness and stability, we introduced a parameter $\alpha$ specified by user. Experimental results obtained from three databases clearly demonstrate that CRLBP ($\alpha=1$) and CRLBP ($\alpha=8$) are insensitive to noise, and both of them can obtain impressive texture classification accuracy.

## Acknowledgment

The authors sincerely thank MVG and Guo for sharing the source codes of LBP and CLBP. This work was supported by the grants of the National Science Foundation of China, Nos. 61175022, 61133010, 31071168, 61005010, 60905023, 61100161, and 60975005, the grant of China Postdoctoral Science Foundation, No. 20100480708 and the grants of the Knowledge Innovation Program of the Chinese Academy of Sciences.

## References

[1] J.G. Zhang, T.N. Tan, Brief review of invariant texture analysis methods, Pattern Recognition 35 (2002) 735–747.
[2] L.S. Davis, Polarograms—a new tool for image texture analysis, Pattern Recognition 13 (3) (1981) 219–223.
[3] J. Duvernoy, Optical digital processing of directional terrain textures invariant under translation, rotation, and change of scale, Appl. Opt. 23 (6) (1984) 828–837.
[4] R.K. Goyal, W.L. Goh, D.P. Mital et al., Scale and rotation invariant texture analysis based on structural property, in: Proceedings of the 1995 IEEE International Conference on Industrial Electronics, Control, and Instrumentation, 1–2, 1995, pp. 1290–1294.
[5] G. Eichmann, T. Kasparis, Topologically invariant texture descriptors, Comput. Vision Graphics Image Process. 41 (3) (1988) 267–281.
[6] R.L. Kashyap, A. Khotanzad, A model-based method for rotation invariant texture classification, IEEE Trans. Pattern Anal. Mach. Intell. 8 (4) (1986) 472–481.
[7] F.S. Cohen, Z.G. Fan, M.A. Patel, Classification of rotated and scaled textured images using Gaussian Markov random field models, IEEE Trans. Pattern Anal. Mach. Intell. 13 (2) (1991) 192–202.
[8] J.L. Chen, A. Kundu, Rotation and gray scale transform invariant texture recognition using hidden Markov model, Icassp-92, International Conference on Acoustics, Speech, and Signal Processing, 1–5, 1992, pp. C69–C72.
[9] R. Porter, N. Canagarajah, Robust rotation invariant texture classification 1997, IEEE International Conference on Acoustics, Speech, and Signal Processing, I–V, 1997, pp.3157–3160.
[10] T. Ojala, M. Pietikainen, T. Maenpaa, Multiresolution gray-scale and rotation invariant texture classification with local binary patterns, IEEE Trans. Pattern Anal. Mach. Intell. 24 (7) (2002) 971–987.
[11] M. Heikkila, M. Pietikainen, C. Schmid, Description of interest regions with center-symmetric local binary patterns, in: Proceedings of Computer Vision, Graphics and Image Processing 4338, 2006, pp. 58–69.
[12] S. Liao, M.W.K. Law, A.C.S. Chung, Dominant local binary patterns for texture classification, IEEE Trans. Image Process. 18 (5) (2009) 1107–1118.
[13] X.Y. Tan, B. Triggs, Enhanced local texture feature sets for face recognition under difficult lighting conditions, IEEE Trans. Image Process. 19 (6) (2010) 1635–1650.
[14] Z.H. Guo, L. Zhang, D. Zhang, A completed modeling of local binary pattern operator for texture classification, IEEE Trans. Image Process. 19 (6) (2010) 1657–1663.
[15] F. Khellah, Texture classification using dominant neighborhood structure, IEEE Trans. Image Process. 19 (12) (2011).
[16] T. Ojala, T. Maenpaa, M. Pietikainen et al., Outex—new framework for empirical evaluation of texture analysis algorithms, in: Proceedings of the 16th International Conference on Pattern Recognition I, 2002, pp. 701–706.
[17] S. Lazebnik, C. Schmid, J. Ponce, A sparse texture representation using local affine regions, IEEE Trans. Pattern Anal. Mach. Intell. 27 (8) (2005) 1265–1278.
[18] K.J. Dana, B. Van Ginneken, S.K. Nayar, et al., Reflectance and texture of real-world surfaces, ACM Trans. Graphics 18 (1) (1999) 1–34.
[19] M. Varma, A. Zisserman, A statistical approach to material classification using image patch exemplars, IEEE Trans. Pattern Anal. Mach. Intell. 31 (11) (2009) 2032–2047.
[20] M. Varma, R. Garg, Locally invariant fractal features for statistical texture classification, in: Proceedings of International Conference on Computer Vision, 2007, pp. 1–8.
[21] M. Varma, A. Zisserman, A statistical approach to texture classification from single images, Int. J. Comput. Vision 62 (1-2) (2005) 61–81.

[22] M. Varma, A. Zisserman, Texture classification: are filter banks necessary? International Conference on Computer Vision and Pattern Recognition, 2003, pp. 691–698.
[23] Y. Xu, H. Ji, C. Fermuller, A projective invariant for texture, International Conference on Computer Vision and Pattern Recognition, 2006, pp. 1932–1939.
[24] Y. Xu, H. Ji, C. Fermuller, Viewpoint invariant texture description using fractal analysis, Int. J. Comput. Vision 83 (1) (2009) 85–100.
[25] Y. Xu, X. Yang, H. Lin, H. Ji, A new texure descriptor using multifractal analysis in multi-orientation wavelet pyramid, International Conference on Computer Vision and Pattern Recognition, 2010, pp. 161–168.
[26] 〈http://www.cfar.umd.edu/~fer/High-resolution-data-base/hr_database.htm〉.

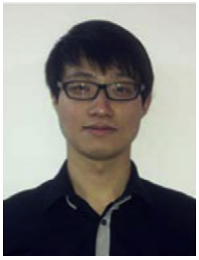

**Yang Zhao** received the B.E. degree from department of automation, University of Science and Technology of China, Hefei, China, in 2008.

From September 2008, he is a Master-Doctoral Program student in department of automation, University of Science and Technology of China, Hefei, China. His research interests include pattern recognition and image processing.

**Wei Jia** received the B.Sc. degree from Central China Normal University, Wuhan, China, in 1998, the M.Sc. degree from Hefei University of Technology, Hefei, China, in 2004, and the Ph.D. degree from University of Science and Technology of China, Hefei, China, in 2008.

He is currently an associate professor in Hefei Institutes of Physical Science, Chinese Academy of Science. His research interests include biometrics, pattern recognition, and image processing.

**Rong-Xiang Hu** received the B.E. degree in Electronic Information Engineering from Hefei University of Technology, Hefei, China, in 2006, and the Ph.D. degree from department of automation, University of Science and Technology of China, Hefei, China.

His research interests include pattern recognition, machine learning and image processing.

**Hai Min** received the B.E. degree from department of automation, Qing Dao University, Qingdao, China, in 2007. the M.S. degree from University of Science and Technology of China, Hefei, China, in 2010.

From September 2010, he is a doctoral Program student in department of automation, University of Science and Technology of China, Hefei, China. His research interests include pattern recognition and image segmentation.